Cement & Concrete Composites 31 (2009) 570–576

Contents lists available at ScienceDirect

Cement & Concrete Composites

journal homepage: www.elsevier.com/locate/cemconcomp

Capillary suction model for characterizing salt scaling resistance of concrete containing GGBFS

D.K. Panesar [a,*], S.E. Chidiac [b]

[a] The University of Toronto, Department of Civil Engineering, 35 St. George Street, Toronto, Ontario, Canada M5S 1A4
[b] McMaster University, Department of Civil Engineering, Center for Effective Design of Structures, 1280 Main Street West, Hamilton, Ontario, Canada L8S 4L7

ARTICLE INFO

Article history:
Received 5 September 2008
Received in revised form 5 January 2009
Accepted 7 January 2009
Available online 20 January 2009

Keywords:
Capillary suction
Chloride binding
Freeze–thaw salt scaling resistance factor
GGBFS
Hydration factor
Ionic sorptivity
Scaling

ABSTRACT

This paper presents a rational method to characterize the freeze–thaw salt scaling performance of concrete based on capillary suction forces. The testing program included evaluating the concrete's chemical chloride binding capacity, degree of hydration, total porosity, compressive strength, sorptivity and de-icer salt scaling resistance conducted at both, 28 days and 2 years. Mixtures consisted of paste and concrete containing 0–60% GGBFS as cement replacement, and a water-to-binder ratio of 0.31 or 0.38. The proposed capillary suction model was adapted to include the concrete's chloride binding capacity, pore characteristics, and age. Results from the capillary suction model are found to correlate with experimentally measured ionic sorption coefficients. Results revealed that the capillary suction depth decreases with increasing percentages of GGBFS due to blocking of capillary pores as a result of the chemical interaction between the saline solution and the binder material. A freeze–thaw salt scaling resistance factor (*F/T SSRF*) is proposed which accounts for the concrete's degree of hydration, sorptivity and tensile strength and is shown to correlate with the concrete's cumulative mass loss tested in accordance with MTO LS-412. Accordingly, the salt scaling performance of concrete containing GGBFS is influenced by the combined effect of the concrete's pore size distribution of the exposed surface, chloride binding capacity, degree of hydration, and tensile strength.

1. Introduction

Freeze–thaw damage in the presence of de-icer salt solution manifests due to the development of pore pressures in hardened cement paste leading to cracking and flaking of the surface layer of concrete. Under laboratory test conditions, concrete containing high percentages of GGBFS (ground granulated blast furnace slag) exhibits greater scaling than OPC (ordinary Portland cement) concrete [1]. Several theories have been proposed to explain the surface scaling damage mechanism of concrete, but they all fail to provide a rationale why concrete containing high ($\geqslant$50) percentages of GGBFS as cement replacement exhibits poorer scaling resistance as compared to concrete with no or lower percentages of GGBFS [1–3]. On the other hand, the use of GGBFS is desirable owing to its economic and environmental benefits given that concrete containing GGBFS as cement replacement can exhibit similar strength, density and homogeneity as OPC concrete by 28 days, as well as improved durability performance against some forms of degradation such as sulfate attack and alkali silica reactions [2,4].

Pore pressure development during freezing and thawing cycles in the presence of de-icing salts is partially attributed to the effect of movement of solution and/or ice formation. The development of pore pressures is influenced by the concrete's microstructural characteristics, namely, total porosity, permeability and the pore size distribution. Concrete containing GGBFS typically exhibits a lower permeability and a lower volume of coarse pores when compared to OPC concrete [2,5]. In comparison to OPC concrete, the chloride ion diffusion coefficient is markedly lower for concrete containing GGBFS due to its relatively denser and discontinuous microstructure and, its relatively higher chloride binding capacity [3,4].

Capillary suction is considered to be the controlling transport property for unsaturated concrete surface. The rate of uptake depends on the pore structure and also the type of sorbing fluid used [6,7]. When concrete is exposed to a chloride solution, the chemical interaction between chloride ions and the binder changes the pore structure of concrete, which results in an overall reduction in total porosity partly due to the blocking of pores with precipitate product from chemical chloride binding reactions [5,8–10]. Previous investigations have shown that changes to the concrete's pore structure after external exposure to chloride solution are reflected in the ionic sorption coefficient [6,7]. The chemical interaction between the binder and the chloride solution also reduces the rate of

* Corresponding author. Tel.: +1 416 946 5712.
E-mail address: d.panesar@utoronto.ca (D.K. Panesar).

0958-9465/$ - see front matter © 2009 Elsevier Ltd. All rights reserved.
doi:10.1016/j.cemconcomp.2009.01.004

ingress as a result of a lower chloride concentration flux [8,11]. The chemical interaction between the binder and the chloride solution also reduces the rate of chloride ingress as a result of a lower chloride concentration flux at different depths from the concrete surface [8,11]. Moreover, good correlation was found to exist between ionic sorptivity and mass loss due to scaling [6,7].

The aim of this study is to provide a rationale to why concrete containing GGBFS exhibits poorer scaling performance as compared to OPC concrete. This study investigates the surface capillary suction as a measure of the load due to freezing and thawing in the presence of de-icer salt, and tensile strength as a measure of resistance of concrete. Accordingly, the influence of GGBFS on the capillary suction is evaluated by examining the concrete's surface pore structure, the ingress of chloride solution and the corresponding mass loss due to de-icer salt scaling.

2. Capillary suction model

For unsaturated concrete at equilibrium, the local relative humidity is influenced by capillary pressure developed by capillary suction and which is related to the capillary pore radius (r_0) and by the osmotic pressure which depends on the concentration of salt solution (C_0) as shown in Eq. (1). In the presence of low ion concentration (3% NaCl), the solution can be considered to behave as an ideal solution [12]:

$$[\ln(RH/100)]_{No\ Binding} = -\frac{v_w^l(1-\chi C_0 v_s^l)\sigma^{l-v}2\cos\theta}{r_0 RT} - \chi n v_w^l C_0 \qquad (1)$$

where, R is the gas constant (J/K mol); T temperature (K); RH relative humidity (%) within a pore; v_w^l molar volume of water in the liquid phase (m^3/mol); σ^{l-v} surface tension of the liquid–vapour interface (N/m); θ wetting angle between pore surface and liquid phase (°); r_0 pore radius (m); $\chi = 10^3$ (L/m^3) is a factor for the unit of concentration to be (mol/L) instead of (mol/m^3); C_0 concentration of salt solution (mol/L); v_w^l molar volume of salt in the liquid phase (m^3/mol); and n the number of moles (2 for NaCl solution).

The chemical interaction between the saline solution and the binder precipitates Friedel's salt within the capillary pores [13–16]. This formation can bar the entry of solution if the pores are clogged or blocked due to the formation of new products. Several studies indicate that consequences of chloride–binder interactions include a more refined pore size distribution, and also an overall reduction in the concrete's total porosity [11,13,14,17,18].

In this study, the effect of chloride binding processes on capillary suction is modeled using the same approach developed for the diffusion coefficient to account for the chloride binding capacity [19,20] where

$$[\ln(RH/100)]_{Binding} = \frac{[\ln(RH/100)]_{No\ Binding}}{V_p B} \qquad (2)$$

Accordingly, the apparent capillary suction, $[\ln(RH/100)]_{Binding}$, is not constant because the chloride binding isotherm is non-linear [21]. V_p is the pore volume fraction (m^3/m^3) and B is a factor that accounts for the influence of chloride binding capacity, $(\frac{\partial c_b}{\partial c_f})$, where, c_f is the free chloride concentration (M), and c_b is the bound chloride (mg chloride/g sample). The chloride binding factor, B, is expected to affect the pore radius and the chloride concentration differently and are defined as B_r and B_c, respectively.

2.1. Influence of chloride on capillary suction

From the capillary suction term in Eq. (1), as the chemical interaction between chloride and binder increases, the capillary pore size decreases [13–16]. In this study, the modified capillary pore radius (r') is represented by:

$$r' = V_P B_r r_0 \qquad (3)$$

and the pore volume fraction is defined as [22]:

$$V_p = (w/b) - 0.19\alpha_{hy} \qquad (4)$$

where w/b is the water to binder ratio and α_{hy} the degree of hydration (%/100).

The factor B_r accounts for the influence of chloride binding capacity on the pore radius. Although the chloride binding capacity includes both physical and chemical binding, research has shown that the chemically bound chloride processes are predominantly responsible for the reduction in pore size [9,11,17,23]. The exact mechanisms that govern the chemical binding of chloride to the hydrated and unhydrated phases are not well defined [24]. For this study, it is assumed that only the unhydrated phases contribute to the alteration of the concrete's pores and the chloride binding factor that affects the pore radius, B_r, is expressed as:

$$B_r = (1-\alpha_{hy})\left(\frac{c_{binding}^{chemical}}{100}\right)\left(\frac{\partial c_b}{\partial c_f}\right) \qquad (5)$$

where the $c_{binding}^{chemical}$ is the contribution of the bound chloride due to chemical processes (%).

2.2. Influence of chlorides on osmotic pressure

The osmotic pressure term in Eq. (1) is also affected by chloride binding processes. As chlorides physically or chemically bind to the cementing material, the free chloride concentration in the pore solution reduces. The modified concentration (C'), is adjusted to account for the volume of pores and the chloride binding capacity:

$$C' = \frac{C_0}{V_P B_c} \qquad (6)$$

B_c is the factor which accounts for the influence of chloride binding on the solution's chloride concentration:

$$B_c = \left(1 + \frac{\partial c_b}{\partial c_f}\right) \qquad (7)$$

By substituting the modified capillary pore radius (r') and the modified concentration (C') as expressed in Eqs. (3) and (6), respectively into Eq. (1), the capillary suction model becomes:

$$[\ln(RH/100)]_{Binding} = -\frac{v_w^l(1-\chi C_0 v_s^l)\sigma^{l-v}2\cos\theta}{(w/b-0.19\alpha_{hy})(1-\alpha_{hy})\left(\frac{c_{binding}^{chemical}}{100}\right)\left(\frac{\partial c_b}{\partial c_f}\right)r_0 RT} - \frac{\chi n v_w^l C_0}{(w/b-0.19\alpha_{hy})\left(1+\frac{\partial c_b}{\partial c_f}\right)} \qquad (8)$$

Eqs. (1) and (8) can be used to evaluate the hydrostatic pore fluid pressure (P) (MPa) [25] by substituting $[\ln(RH/100)]$ for either the 'no binding' or 'binding' case, respectively, in the following equation:

$$P = p'' - p' = \frac{[\ln(RH/100)]RT}{v_w^l(1-\chi C_0 v_s^l)} \qquad (9)$$

where, p'' is the vapour pressure, and p' the pore fluid pressure.

Capillary suction depth, ψ (m), is then evaluated from:

$$\psi = \frac{P}{g\rho} \qquad (10)$$

where g is the gravity constant (9.81 m/s^2), ρ the solution density (1017 kg/m^3 for 3% NaCl solution), and P the pressure evaluated from Eq. (9).

3. Experimental study

Experiments were conducted on paste and concrete samples. Paste samples were used to evaluate the degree of hydration, chloride binding capacity, and percentage of chemically bound chloride. The concrete samples were used to evaluate the compressive strength, sorption coefficient, and freeze–thaw salt scaling resistance.

The primary mix design variables considered in this study include the percentage of GGBFS as cement replacement (0–60%), w/b ratio (0.31 or 0.38), and age of the concrete (28 days or 2 years). Table 1 presents the chemical composition of the materials. Tables 2 and 3 provide the mix design proportions for the paste and dry cast concrete, respectively. The nominal maximum coarse aggregate size is 13 mm.

3.1. Degree of hydration

The paste mix procedure, sample preparation, curing regime and details regarding the non-evaporable water content measurement procedure are detailed in [26]. Fig. 1 shows the influence of w/b ratio and the percentage of GGBFS on the evolution of non-evaporable water content from day 28 to 2 years.

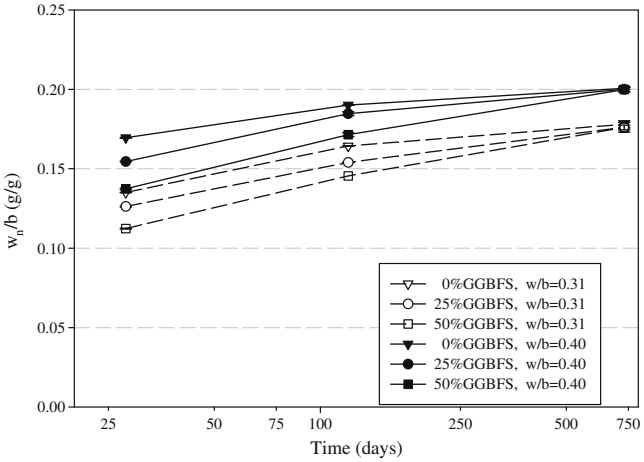

Fig. 1. Evolution of non-evaporable water content from 28 days to 2 years.

The non-evaporable water content or chemically combined water provides an indirect means to evaluate the degree of hydration (α_{hy}) (%) [27]:

$$\alpha_{hy} = \frac{w_n/b}{k} * 100 \tag{11}$$

where k (g/g) is the mass of chemically combined water needed to fully hydrate one gram of cement and w_n/b (g/g) is the mass of non-evaporable water per ignited mass of cementing material. The constant 'k' depends on the cement composition, but is typically shown to range from 0.23 to 0.25 (g/g) for OPC paste [28–30].

A study conducted by Mills [29] reported the non-evaporable water content at ultimate hydration of ball-milled slurries which contained varying amounts of GGBFS as cement replacement. The measured non-evaporable water contents were based on oven drying the samples at 110 °C and furnace ignition at 1000 °C. The ultimate chemically combined water at full hydration, k, was reported to be 0.253, 0.255 and 0.266 (g/g) for slurries with 0%, 25% and 50% GGBFS, respectively [29]. Mills considered the values to be reliable estimates of the chemically combined water at full hydration and are adopted in this study to estimate the degree of hydration based on Eq. (11). The degree of hydration reported in Table 4 are the mean values of three measurements. The corresponding coefficient of variation for all of the data reported in Table 4 is less than 2%.

3.2. Chloride binding capacity

The mix procedure, sample preparation, and chloride binding test method of the paste samples are detailed in Chidiac et al. [11]. The constants α and β of the chloride binding isotherms fit to a Freundlich form of:

$$c_b = \alpha c_f^{\beta} \tag{12}$$

are summarized in Table 5 along with the corresponding coefficient of determination. The chloride binding capacity is evaluated at a

Table 1
Chemical composition of OPC and GGBFS.

Constituent	OPC (%)	GGBFS (%)
SiO_2	20.1	34.0
Al_2O_3	5.1	11.1
Fe_2O_3	2.3	0.5
CaO	63.6	36.6
MgO	2.5	11.6
SO_3	3.0	3.3
K_2O	–	0.5
Na_2O	–	0.5
TiO_2	–	0.7
Mn_2O_3	–	1.3

Table 2
Paste mix design proportions.

OPC:GGBFS	OPC (%)	GGBFS (%)	w/b ratio
4:0	100	0	0.31
3:1	75	25	0.31
2:2	50	50	0.31
4:0	100	0	0.40
3:1	75	25	0.40
2:2	50	50	0.40

Table 3
Concrete mix design composition.

OPC:GGBFS	Total binder (kg/m^3)	OPC (kg/m^3)	GGBFS (kg/m^3)	Fine aggregate (kg/m^3)	Coarse aggregate (kg/m^3)	w/b
4:0	360	360	0	1253	835	0.31
3:1	360	270	90	1249	833	0.31
3:2	450	270	180	1156	771	0.31
2:2	360	180	180	1246	831	0.31
2:3	450	180	270	1152	768	0.31
4:0	360	360	0	1275	847	0.38
3:1	360	270	90	1257	843	0.38
2:3	450	180	270	1204	808	0.38
2:2	360	180	180	1257	843	0.38
3:2	450	270	180	1204	808	0.38

Table 4
Estimated degree of hydration (α_{hy}).

%GGBFS	w/b ratio	28 day mean α_{hy} (%)	2 year mean α_{hy} (%)
0	0.31	53	70
25	0.31	49	69
50	0.31	43	67
0	0.40	67	79
25	0.40	61	78
50	0.40	53	77

Table 5
Chloride binding capacity based on fit Fruendlich isotherm at 0.5 M total initial chloride concentration.

% GGBFS	α	β	R^2	c_f (M)	$(\partial c_b/\partial c_f)$
0	8.98	0.4263	0.98	0.4278	6.23
25	9.08	0.3811	0.99	0.4138	5.97
50	10.01	0.4555	0.96	0.4339	7.18
60	10.05	0.4466	0.98	0.4301	7.16

total chloride concentration of 0.5 M. The average free chloride content reported in Table 5 is based on three samples which have coefficients of variation less than 5%.

The percentage of chemically bound chloride for 0% and 40% GGBFS paste corresponding to a total chloride concentration of 0.5 M are given in Chidiac et al. [11]. In this study, the percentage of chemically bound chloride for concrete containing 25% is estimated by linear interpolation between the measured data for 0% and 40% GGBFS mixtures. For percentages of GGBFS greater than 40%, the percentage of chemically bound chloride is assumed to be equal to the measured value for concrete containing 40% GGBFS. This assumption is made because at high percentages of GGBFS (>50%), small differences in chloride binding have been observed. This could be attributed to the limited sites available for chloride binding, either physical pore space or species required for the chloride to chemically react [31].

3.3. Tensile strength

The predicted tensile strength, f_t, are based on ACI-363 [32] for high strength concrete:

$$f_t = 0.6\sqrt{f'_c} \quad \text{for } 21\text{ MPa} < f'_c < 83\text{ MPa} \tag{13}$$

In this study, it is assumed that the estimated tensile strength of the bulk concrete is equal to that of the concrete's cover layer. The measured compression test data is summarized in Table 6. Use of the reported strengths in this study assumes that the compressive strengths, f'_c, tested at 4 months are equivalent to the 2 year strengths and are used to estimate the concrete's tensile strength as reported in Table 6.

3.4. Sorption

The sorption coefficient referred to as sorptivity, was evaluated in accordance with ASTM C 1585-04 [33] using two sorbing fluids, distilled water (DW) and 3% NaCl solution and the results are shown in Fig. 2. This study presents the sorptivity for concrete with a w/b of 0.31 at 28 days and a w/b of 0.38 at 2 years. The specimens were stored and tested in an environment of a relative humidity (RH) of 55%, and a temperature of 23 ± 2 °C.

Table 6
Compressive strength measurements and tensile strength estimates.

% GGBFS	w/b ratio	Age	Measured compressive strength		Estimated tensile strength (MPa)
			Mean (MPa)	COV (%)	
0	0.31	28 days	62	6.4	4.7
25	0.31	28 days	66	7.5	4.9
40	0.31	28 days	71	2.8	5.1
60	0.31	28 days	65	1.5	4.8
0	0.38	4 months	74	2.7	5.2
25	0.38	4 months	89	4.5	5.7
40	0.38	4 months	86	1.2	5.6
60	0.38	4 months	78	9.0	5.3

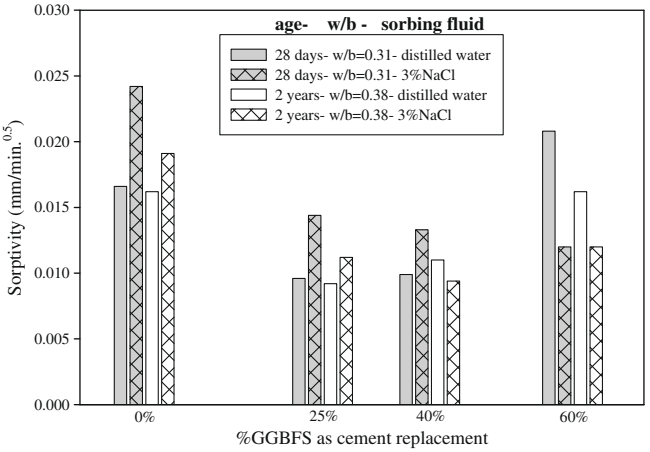

Fig. 2. Measured sorptivity coefficients based on two sorbing fluids, distilled water and 3% NaCl solution [6].

3.5. Scaling resistance

Fig. 3 presents the de-icer salt scaling resistance reported as the cumulative mass loss after 50 freeze–thaw cycles tested in accordance with MTO LS-412 [34]. This study presents the scaling data for concrete containing a w/b of 0.31 at 28 days and a w/b of 0.38 at 2 years.

4. Results

4.1. Capillary suction model

Figs. 4 and 5 show the [ln(*RH*/100)], which is linearly proportional to the capillary pore pressure, as a function of pore size for 28 day and 2 year old concrete, respectively. The results are based on a NaCl concentration of 0.5 M which is of interest because it represents the concentration prescribed in MTO LS-412 [34].

The curve computed based on Eq. (1) shown in Figs. 4 and 5 does not include the effect of chloride binding processes on the capillary suction and is therefore the same for all concrete mixtures. For both the 'binding' and 'no binding' cases, [ln(*RH*/100)] increases with pore diameters ranging from 0.01 to 0.5 μm. The curves in Figs. 4 and 5 computed based on Eq. (8) are specific for a particular concrete mixture because it accounts for degree of hydration, chloride binding capacity, pore volume data, and the

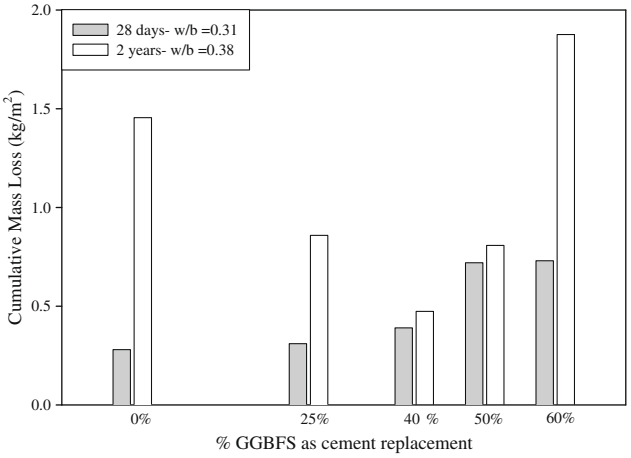

Fig. 3. Scaling resistance tested in accordance with MTO LS-412 [6].

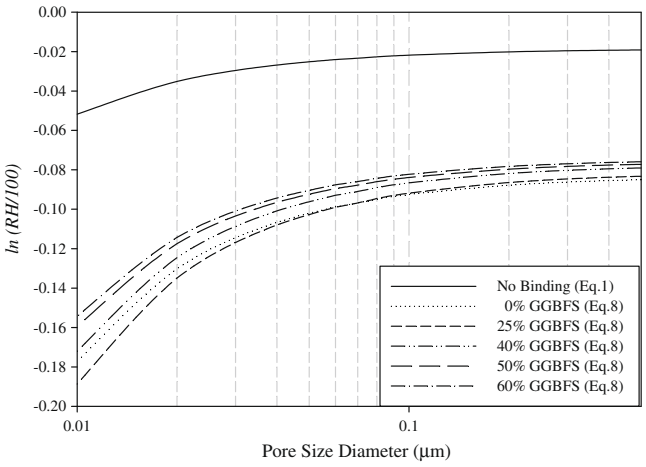

Fig. 4. Influence of GGBFS using the capillary suction model and data for 28 day concrete with a w/b of 0.31 exposed to 0.5 M initial chloride concentration.

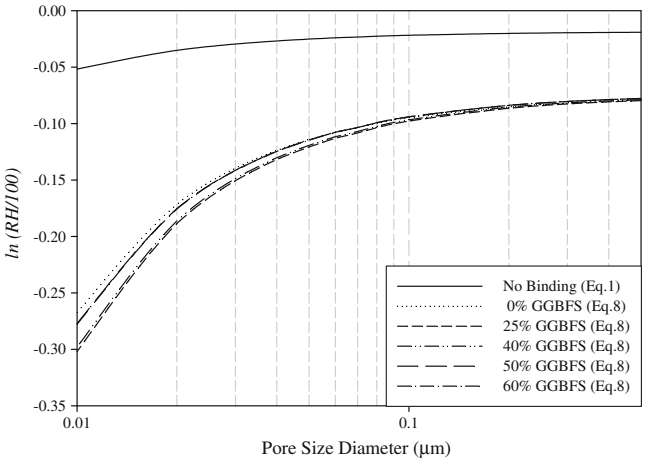

Fig. 5. Influence of GGBFS using the capillary suction model and data for 2 year old concrete with a w/b of 0.38 exposed to 0.5 M initial chloride concentration.

constant values given in Table 7. The results of Figs. 4 and 5 show that capillary pore pressures increase for all concrete mixtures when the interaction between the chlorides and the paste is accounted for. This increase in pressure is attributed to the reduction in pore size as described in Section 2. Considering the effect of chloride binding, the pressures within the capillary pore size regions, 0.1–1 μm, are constant and similar for all mixtures and increase slightly towards the 0.1 μm capillary pore size as shown in Figs. 4 and 5. In the finer capillary pore region, 0.01–0.1 μm, the pore pressures, evaluated from Eq. (8), do discriminate between the different mixtures.

Table 7
Constants used in Eqs. (1) and (8) [12].

Variable	Value	Units
v_w^l	1.80E−05	m^3/mol
θ	30	degrees
σ^{l-v}	0.076	N/m
χ	1000	L/m^3
n	2	
v_s^l	2.13E−05	m^3/mol
C_0	0.513	mol/L
R	8.314	J/kmol
T	295	K
$\rho_{3\%\ NaCl\ 22C}$	1017	kg/m^3

Table 8
Representative pore size, total porosity and porosity factor (*PF*).

% GGBFS	Average pore diameter (μm)		Total porosity (%)		Porosity factor (*PF*)
	Exposure solution		Exposure solution		
	Distilled water	3% NaCl	Distilled water	3% NaCl	
0	0.0451	0.0460	7.5	6.8	1.00
25	0.0419	0.0389	6.9	6.7	0.93
40	0.0390	0.0367	6.4	5.9	0.85
60	0.0353	0.0285	5.7	4.8	0.76

Evaluation of the hydrostatic pressure based on Eq. (9) requires a representative pore size for each mixture. The average pore size diameter is evaluated from the pore size distributions reported in Chidiac et al. [11]. In this study, the representative pore diameter is assumed to correspond to the pore diameter found at 50% of the cumulative pore volume. Table 8 presents the representative pore diameters for each mixture after exposure to distilled water or 3% NaCl solution. The results show that after exposure to 3% NaCl solution the representative pore diameter is smaller in comparison to those exposed to distilled water, with the exception of the 0% GGBFS mixture in which case the diameters are similar. The representative pore diameter decreases with increasing percentages of GGBFS indicating that concrete containing increasing percentages of GGBFS have a greater fraction of smaller diameter capillary pores.

4.1.1. Porosity factor

Normalization factor, referred to as the porosity factor, *PF*, is introduced to account for the relative differences between the total porosity of the various concrete mixtures. The porosity factor is deemed necessary to relate capillary uptake to sorptivity, since sorptivity is influenced by the total capillary pore volume and not a single pore. The pressures determined from Eq. (9) are factored to reflect the influence of GGBFS on the total porosity. The porosity factor is defined as:

$$PF = \frac{actual\ porosity\ of\ mixture}{porosity\ of\ 0\%\ \text{GGBFS}\ concrete\ mixture} \tag{14}$$

Table 8 presents the total porosity, and the porosity factor for all mixtures. The effect of chloride solution on the capillary suction is evaluated as the difference in pressure determined from Eqs. (1) and (8) factored by *PF*.

4.2. Sorption coefficient

Fig. 2 shows the influence of sorbing fluid on the sorption coefficient for each concrete mixture. The results show that using 3% NaCl as a sorbing fluid does not have the same effect on the rate of solution uptake for all of the concrete mixtures. For 0% GGBFS, the presence of 3% NaCl solution increases the rate of uptake whereas for concrete containing 60% GGBFS, the presence of 3% NaCl decreases the rate of uptake as compared to the rate of uptake of distilled water.

The influence of chloride ions on the rate of capillary uptake is determined by calculating the difference between the sorption coefficient determined when distilled water is used as a sorbing fluid and the sorption coefficient when 3% NaCl solution is used as a sorbing fluid. This property is referred to as the 'ionic sorptivity' [6,7].

4.3. Model validation

Fig. 6 shows a linear correlation between the experimentally determined ionic sorption coefficients and the computed capillary

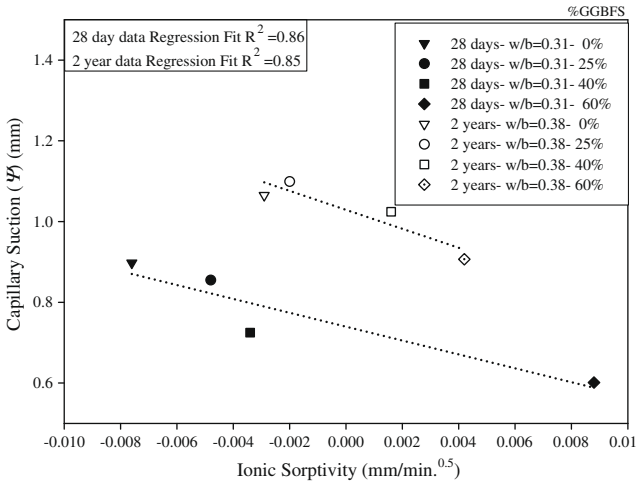

Fig. 6. Correlation between experimentally determined sorptivity and computed capillary suction from Eq. (10) using factored pressure [PF* ($P_{No\ Binding}$ – $P_{Binding}$)] based on Eqs. (1) and (8).

suction based on the isolated effect of the interaction between the chloride solution and the cement paste. The effect of physical and/or chemical binding on the capillary suction is determined as the difference between the, $P_{No\ Binding}$ calculated from Eq. (1) and $P_{Binding}$ based on Eq. (8). The fit regression lines for the 28 day and 2 year data have a similar coefficient of determination (R^2) (0.85,0.86). Although the slopes of the regression lines are somewhat similar, the spread of ionic sorptivity and capillary suction results are narrower for the 2 year old concrete as compared to the 28 day data. This could be attributed to the fact that at 2 years, the degree of hydration is essentially the same for all mixtures, as shown in Table 4, and is therefore not an influencing variable. In comparison, at 28 days, the degree of hydration ranges from 43% to 53% and is influenced by the GGBFS content. In addition, the data for the concrete presented at 28 days also has a lower w/b ratio as compared to the concrete used for the 2 year data. As a result, one would expect a difference in capillary pore structure which would also contribute to the shift in the two curves shown in Fig. 6.

For both ages of concrete, 28 days and 2 years, the correlation shows that with increasing percentages of GGBFS, the capillary suction depth decreases due to the effect of chloride solution. This corresponds to a decreasing ionic sorption coefficient. The negative ionic sorptivity in Fig. 6 means that the rate of uptake of 3% NaCl solution exceeds the rate of uptake of distilled water. This is consistent with Eq. (1) which shows that the capillary force of a solution consists of the superimposed effect of the capillary suction flux and the chloride ion concentration gradient flux. The greatest additive response of the two fluxes is observed for concrete containing 0% GGBFS and is reflected by negative ionic sorptivities shown in Fig. 6.

The ionic sorptivity becomes increasingly positive when the rate of ingress of 3% NaCl solution is less than the rate of ingress of distilled water. In this case, the additive effect of the two fluxes shown in Eq. (1) is not observed. This response is attributed to the interaction between the chloride solution and the binder material on the capillary uptake pressure which is captured in Eq. (8).

5. Ionic sorptivity and the de-icer salt scaling resistance

Many of the commonly proposed scaling damage mechanisms attribute frost damage to the freezing and expansion of water within a pore and the forced movement of solution in attempt to relieve the free energy and/or the chloride ion concentration gradient [2,35,36]. Hydraulic pressure is controlled by the degree of saturation of a capillary cavity and the pressure developed due to the movement of the pore solution, which is in part controlled by the permeability of the concrete's microstructure [36,37]. A negative ionic sorption coefficient indicates that the ingress of chloride solution exceeds the ingress of distilled water which corresponds to a higher degree of saturation of the capillary cavity. In contrast, a positive ionic sorption coefficient indicates that the uptake of chloride solution is less than the uptake of distilled water. The response is expected to be partly due to chloride–binder interactions which block the surface of the capillary pores resulting in solution trapped beneath the surface, creating a saturated cavity. When subjected to freezing temperatures, the water will expand and the brine solution will move towards the outer surface of the concrete in attempt to relieve the free energy gradient. Both the expansion of water and the movement of solution generate pore pressures. The magnitude of the pressure depends on the degree of saturation. In this regard it is postulated that ionic sorptivity is a measure of the degree of saturation. For instance, a high degree of saturation can be reflected by either a high positive ionic sorptivity or a high negative sorptivity. Thus, ionic sorptivity provides a measure of the load due to pore pressures, and the tensile strength provides a measure of the concrete's resistance. Accordingly, a new freeze–thaw salt scaling resistance factor (*F/T SSRF*) is proposed:

$$F/T\,SSRF = Hydration\ Factor\left(\frac{Ionic\ Sorptivity}{Tensile\ Strength}\right) \tag{15}$$

The 'hydration factor' is introduced to account for the w/b ratio and age of the concrete as given in Eq. (16) [38].

$$Hydration\ Factor = \frac{\log age}{\log 28}\left[\frac{\alpha_{age}^{w/b=0.4}}{\alpha_{age}^{w/b=0.31}} + \frac{\alpha_{age}^{w/b=0.4}}{\alpha_{28\ days}^{w/b=0.4}}\right] \tag{16}$$

where *age* reflects the concrete's age and is measured in days. It should be noted that the hydration factor of unity corresponds to a 28 day concrete with a w/b ratio of 0.31.

The correlation between the cumulative scaling mass loss after 50 freeze–thaw cycles and the ratio of the *F/T SSRF* is shown in Fig. 7. By comparing the scaling acceptance limit of 0.8 kg/m^2 specified by OPSS 1351 (2002) [39], and the freeze–thaw salt scaling test results, limits were derived for *F/T SSRF* and are represented by the following relation:

$$-0.0018 \le F/T\,SSRF \le +0.002 \tag{17}$$

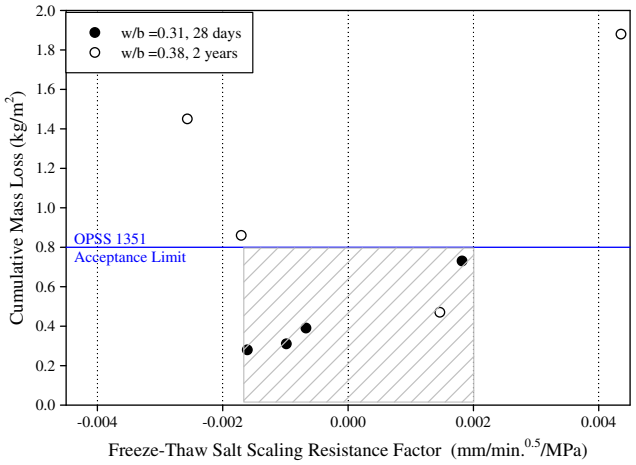

Fig. 7. Correlation between scaling resistance and freeze–thaw salt scaling resistance factor (*F/T SSRF*) (scaling acceptance limit specified by OPSS 1351 shown at 0.8 kg/m^2).

Use of the *F/T SSRF* in conjunction with the acceptance limits of Eq. (17) provide the basis to develop an effective, inexpensive, and quick evaluation of concrete's susceptibility to freeze–thaw salt scaling.

6. Conclusions

The main findings from this study are:

1. A capillary suction model is developed which accounts for the interplay between the binder's chloride binding capacity, changes to the physical microstructure due to exposure to chlorides, and age. The model results are linearly correlated to experimental ionic sorptivity data for concrete containing 0–60% GGBFS as cement replacement at 28 days and 2 years.
2. The chloride capillary suction depth decreases with increasing percentage of GGBFS owing to the blocking of capillary pores by precipitate from chemical binding reactions.
3. A new property, ionic sorptivity, is introduced and reflects the difference between the sorption coefficients evaluated using distilled water as a sorbing fluid and 3% NaCl as a sorbing fluid. Ionic sorptivity indirectly provides a measure of hydraulic pressure.
4. A *F/T SSRF* which is a function of the hydration factor, ionic sorptivity, and tensile strength is proposed to characterize the scaling resistance of concrete. It provides an effective and quick evaluation of the concrete resistance to freeze–thaw scaling compared to MTO LS-412 results.

Acknowledgements

This study forms a part of ongoing research at The McMaster University's Centre for Effective Design of Structures funded through the Ontario Research and Development Challenge Fund. This research was also funded through grants from the Natural Science and Engineering Research Council of Canada (NSERC), Ontario Concrete Pipe Association, Cement Association of Canada, and Ontario Centres of Excellence – MMO.

References

[1] Panesar DK, Chidiac SE. Multi-variable statistical analysis for scaling resistance of concrete containing ground granulated blast furnace slag. Cem Concr Comp 2007;29:39–48.
[2] Copuroglu O. Frost salt scaling of cement-based materials with a high slag content. Ph.D. Dissertation, Delft, Technical University of Delft; 2006.
[3] Bleszynski R, Hooton RD, Thomas DA, Rogers CA. Durability of ternary blend concrete with silica fume and blast-furnace slag: laboratory and outdoor exposure site studies. ACI Mater J 2002;99(5):499–508.
[4] Chen W. Hydration of slag cement – theory modeling and application. Ph.D. Dissertation, The Netherlands, University of Twente; 2006.
[5] Luo R, Cai Y, Wang C, Huang X. Study of chloride binding and diffusion in GGBS concrete. Cem Concr Res 2001;33:1–7.
[6] Chidiac SE, Panesar DK. Sorptivity of concrete as an indicator of laboratory freeze–thaw scaling performance. In: International RILEM workshop on performance based evaluation and indicators for concrete durability, Madrid, Spain; 2007. p. 59–66.
[7] Chidiac SE, Zibara H. Dry-cast concrete masonry products: properties and durability. Can J Civil Eng 2007;34:1413–23.
[8] Suryavanshi AK, Scantlebury JD, Lyon SB. Mechanisms of Friedel's salt formation in cements rich in tri-calcium aluminate. Cem Concr Res 1996;26(5):729–41.
[9] Suryavanshi AK, Swamy RN. Influence of penetrating chlorides on the pore structure of structural concrete. Cem Concr Agg 1998;20:169–79.
[10] Tumidajski PJ, Chan GW. Boltzmann-Matano analysis of chloride diffusion in to blended cement concrete. J Mater Civil Eng 1996:195–200.
[11] Chidiac SE, Panesar DK, Zibara H. Chloride binding and its effects on the pore structure of concrete containing GGBFS. Cem Concr Res, submitted for publication.
[12] Rijniers L. Salt crystallization in porous materials: an NMR study. Ph.D. Dissertation, The Netherlands, Technical University of Eindhoven; 2004.
[13] Boddy A, Bentz E, Thomas MDA, Hooton RD. An overview and sensitivity study of a multimechanistic chloride transport model. Cem Concr Res 1999;29:827–37.
[14] Ababneh A, Benboudjema F, Xi Y. Chloride penetration in non-saturated concrete. J Mater Civil Eng 2003:183–90.
[15] Ollivier JP, Arsenault J, Truc O, Marchand J. Determination of chloride binding isotherm from migration tests. In: Mehta PK, editor. Proceedings of the Mario Collepardi symposium on advances in concrete science and technology; 1997. p. 195–217.
[16] Dhir RK, Hewlett PC, Byars EA, Bai JP. Estimating the durability of concrete in structures. Concrete 1994:25–30.
[17] Beaudoin JJ, Ramachandran VS, Feldman RF. Interaction of chloride and C–S–H. Cem Concr Res 1990;20:875–83.
[18] Suryavanshi AK, Scantlebury JD, Lyon SB. The binding of chloride ions by sulfate resistant Portland cement. Cem Concr Res 1995;25(3):581–92.
[19] Nokken M, Boddy A, Hooton RD, Thomas MDA. Time dependent diffusion in concrete-three laboratory studies. Cem Concr Res 2004;36:200–7.
[20] Neithalath N. Analysis of moisture transport in mortars and concrete using sorption–diffusion approach. ACI Mater J 2006;103(3):209–17.
[21] Tang L, Nilsson L-O. Chloride binding capacity and binding isotherms of OPC pastes and mortars. Cem Concr Res 1993;23:247–53.
[22] Tang L, Nilsson L-O. Chloride binding isotherms – an approach by applying the modified BET equation. In: Nilsson L-O, Ollivier J-P editors. RILEM proceeding chloride penetration into concrete; 1995. p. 36–42.
[23] Haque MN, Kayyali OA. Free and water-soluble chloride in concrete. Cem Concr Res 1995;25:531–42.
[24] Zibara H. Binding of external chlorides by cement pastes. Ph.D. Dissertation, Toronto, University of Toronto; 2001.
[25] Grasley ZC, D'Ambrosia MD, Lange DA. Internal relative humidity and drying stress gradients in concrete. Mater Struct 2006;39(9):901–9.
[26] Chidiac SE, Panesar DK. Evolution of mechanical properties of concrete containing ground granulated blast furnace slag and effects on the scaling resistance at 28 days. Cem Concr Comp 2008;30(2):63–71.
[27] Neville AM, Brooks JJ. Concrete Technology. UK.: John Wiley & Sons Inc., Longman Scientific & Technical; 1987.
[28] Powers TC, Brownyard TL. Studies of the physical properties of hardened Portland cement paste. Portland Cem Assoc Bull 1948:22.
[29] Mills RH. Factors influencing cessation of hydration in water cured cement pastes. In: Symposium on structure of Portland cement paste and concrete, special report 90. Highway Research Board Division of Engineering, National Research Council; 1966. p. 406–24.
[30] Taylor HFW. Cement chemistry. San Diego CA: Academic Press; 1990.
[31] Wowra O, Setzer MJ. Sorption of chlorides on hydrated cement and C3S pastes. In: Setzer MJ, Auberg R, editors. Frost resistance of concrete. London: E&FN Spon; 1997. p. 147–53.
[32] American Concrete Institute, State-of-the-art report on high-strength concrete. ACI Committee Report 363, Detroit; 1992 (Reapproved 1997). p. 1–55.
[33] American Society for Testing and Materials. Standard test method for measurement of rate of absorption of water by hydraulic cement concretes' ASTM C 1585-04; 2004. p. 772–6.
[34] Ministry of Transportation Ontario. Method of test for scaling resistance of concrete surfaces exposed to de-icing chemicals (MTO LS-412)' Rev. No. 17; August 1997. 5p.
[35] Valenza J, Scherer GW. Mechanism for salt scaling. J Am Cer Soc 2006;89(4):1161–79.
[36] Pigeon M, Pleau R. Durability of concrete in cold climates. Modern concrete technology, vol. 4. E&FN Spon; 1995.
[37] Powers TC. Freezing effects in concrete. Durability of concrete. Detroit: ACI Publication SP-47; 1975. p. 1–11.
[38] Espinosa RM, Franke L. Influence of the age and drying process on pore structure and sorption isotherms of hardened cement paste. Cem Concr Res 2006;36:1969–84.
[39] Ontario Provincial Standard Specifications. Material specification for precast reinforced concrete catch basins, manholes, ditch inlets and valve chambers. OPSS-1351; March 1991 (OCPA Draft 1 July 6, 2002, OPSS-1351). 8p.